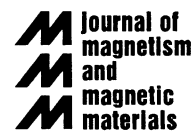




ELSEVIER

Journal of Magnetism and Magnetic Materials 225 (2001) 262–276



www.elsevier.com/locate/jmmm

Magnetic design considerations for devices and particles used for biological high-gradient magnetic separation (HGMS) systems

Gareth P. Hatch^{a,*}, Richard E. Stelter^b

^aDexter Magnetic Technologies, 1050 Morse Avenue, Elk Grove Village, IL 60007, USA

^bDexter Magnetic Technologies, 48460 Kato Road, Fremont, CA 94538, USA

Abstract

An overview of the magnetic systems used in biological high-gradient magnetic separation (HGMS) is presented. The magnetic design parameters of a range of separation devices are discussed. Such designs have distinct magnetic field characteristics and are usually tailored to meet the needs of particular protocols. The various types of magnets and particles are also discussed, with a comparison of materials available and their magnetic properties. © 2001 Elsevier Science B.V. All rights reserved.

Keywords: Magnetic design; Separator design; Quadrupole; Force density; Flux density calculations; Magnetic separation; Magnetic beads; High gradient

1. Introduction

In recent years, the use of high-gradient magnetic fields for separation has become widespread in the fields of biology, biotechnology and other bio-medical disciplines. Applications include cell sorting, RNA and DNA isolation, preparation, purification and sequencing, as well as immunology and a wide variety of isolation techniques for biological entities.

The two key magnetic components of such systems are the magnetic particles used in the separation of the biological entities, and the magnetic

field used to separate them. Such a field is usually generated by the presence of permanent magnets, while some devices use electromagnets to achieve the same aim — the generation of a static magnetic field with a significant field gradient, within the target volume. Simple magnet blocks typically generate field gradients in the order of $1\text{--}6 \text{ Tm}^{-1}$ across the diameter of standard 15–50 ml laboratory test tubes. High-gradient magnet separators [HGMS] generate field gradients that are significantly higher than this, through the use of optimally designed magnetic circuits. Across 15–50 ml test tubes, such systems may generate gradients ranging from 10 to 100 Tm^{-1} . Even higher gradients can be achieved with smaller bore containers and separator systems.

While simple ‘off-the-shelf’ magnets can be used in the separation process, the field produced can be

* Corresponding author. Tel.: +1-847-956-1140; fax: +1-847-956-8205.

E-mail address: ghatch@dextermag.com (G.P. Hatch).

significantly optimized by the system designer, through the careful tuning of the key parameters of the system. These parameters include magnet material, geometry, configuration and initial magnetization. These parameters will directly affect the separation time, total yield of target entities, target retention, and integrity of the target entities.

In addition, selection of the magnetic particles based on material, shape, size and size distribution will significantly affect the end separation results. The present work seeks to outline a number of the above factors and how the system designer uses them to give the end user what they want — an optimized HGMS system.

2. Permanent magnets

Most commercially available HGMS systems consist of an array or other configuration of permanent magnets. System designers need to consider the properties of magnetic materials when using them in a HGMS system. The most common material groups are listed together with their key characteristics in Table 1.

Most commercially available magnetic separation systems utilize high-energy Nd–Fe–B material to generate as much magnetic flux as possible for a given volume of material. Nd–Fe–B has some disadvantages over other materials however; it has poor corrosion resistance and so should be coated and sealed into its housing to prevent corrosion through standard cleaning regimens. Its other disadvantage is that it is sensitive to temperature — magnetic materials generally do not react favorably to temperature (there are some exceptions), since the additional thermal energy will begin to

negate the mechanism present for projecting an external magnetic field. Nd–Fe–B magnets may need to be re-magnetized after being exposed to temperatures higher than 150°C, depending on magnet geometry.

The advantages of Nd–Fe–B far outweigh the disadvantages however, in normal room temperature applications. By shaping magnets with particular orientations, such magnets can be configured to push flux out into the working volume of an assembly with little difficulty. Such configurations are only possible due to the ability of Nd–Fe–B (and Sm–Co) to resist strong demagnetizing fields (in this case, the external magnetic fields of other magnets in the vicinity).

3. Fundamentals of magnetism

Nd–Fe–B is an obvious example of a ferromagnetic material. While ferromagnetism is the most commonly known form of magnetism, there are other types of magnetic behavior that are particularly relevant to HGMS separation systems, and the particles used within them. The designer can use these characteristics to determine the appropriate particles for use within a system.

In magnetic materials, a magnetic field is produced because of the movement of electrons within the material, which produces the field around the material and a magnetization effect within it. An electrical charge moving through a conductor will also produce a magnetic field; therefore the magnetic field strength H can be measured in Am⁻¹ [SI units are used throughout the present work]. When a material experiences a magnetic field, the individual atomic moments contribute to the overall

Table 1
Comparison of key characteristics of commercially available magnetic materials

Characteristic	Ceramic	Alnico	Bonded Nd–Fe–B	Sm–Co	Nd–Fe–B
Highest energy product BH_{\max} (kJm ⁻³)	32	59	79	254	382
Maximum operating temperature (°C)	300	550	150	300	150
Resistance to demagnetization	Moderate	Low	High	Very high	High
Corrosion resistance [uncoated]	Excellent	Excellent	Good	Good	Poor
Mechanical toughness	Moderate	Tough	Moderate	Very brittle	Brittle
Relative cost	Very low	Moderate	High	Very high	High

response of that material to the field. This response is called the magnetic induction \mathbf{B} and is an inherent property of the material; it is also known as the flux density and is measured in tesla (T).

The relationship between the applied field and the response of the material is known as the permeability of the material μ . In free space

$$\mu_0 = \frac{B}{H} \quad (1)$$

and the permeability of free space $\mu_0 = 4\pi \times 10^{-7} \text{ WbA}^{-1} \text{ m}^{-1}$. In any other medium, however, the permeability μ may not be a linear function of H ; although

$$\mathbf{B} = \mu \mathbf{H} \quad (2)$$

μ may vary with the applied magnetic field, particularly in ferromagnetic materials. In order to relate the magnetic properties of a material to the magnetic induction caused by an applied field, the magnetization \mathbf{M} can be defined as follows:

$$\mathbf{M} = \frac{\mathbf{m}}{V}, \quad (3)$$

where \mathbf{m} is the magnetic moment and V is the volume of the material. The unit mass magnetization can be defined in a similar fashion.

In the presence of an external magnetic field

$$\mathbf{B} = \mu_0(\mathbf{H} + \mathbf{M}). \quad (4)$$

This equation is true for all magnetic systems.

Finally, the susceptibility χ of a material can be defined as

$$\chi = \frac{M}{H}. \quad (5)$$

A seldom-mentioned fact is that all materials exhibit magnetic properties to some extent at all times, depending on their atomic structure and temperature. Some, like iron, cobalt and nickel can exhibit strong external magnetic fields under certain conditions. Others display little magnetism (paramagnetic) or are slightly antimagnetic (diamagnetic).

With no external influence, atomic magnetic moments align themselves in their least-energy state and cancel each other internally so a material dis-

plays no net magnetic poles (and thus, no external magnetic field). Atomic magnetic moments are partially the result of electron orbits, so as temperature rises and the orbital path lengthens the strength of the magnetic moment decreases. The other factor in the strength of the atomic magnetic moment is chemistry and the balance of electrons in the shells of the atom. The chemistry of the material establishes how the electron shells are filled, so certain alloys of normally magnetic materials can be non-magnetic (e.g. monel) while other ‘non-magnetic’ materials can be combined in ways to allow them to develop substantial magnetic moments.

Since magnetism originates at the atomic level, from the state of a particular material’s electrons, all materials fall into one of five major groups, namely, ferromagnetic, antiferromagnetic, ferrimagnetic, diamagnetic and paramagnetic. Ferromagnetism, antiferromagnetism and ferrimagnetism are ordered states; diamagnetism and paramagnetism are transient states that exist as a result of an applied magnetic field.

3.1. Ferromagnetism

On a microscopic scale, ferromagnetic materials exhibit magnetism even without an applied field. The atomic moments align parallel to each other, because of an exchange interaction between electrons — there is a significant imbalance in the electron bands of coupled atoms, and there is therefore a large spontaneous magnetization present. This is typically 10^4 larger than the field generated by the total magnetic moment of the ferromagnetic materials.

Weiss postulated the mean-field theory for ferromagnetic materials [to be found in any standard text on the subject], based on the idea that atomic magnetic moments were aligned parallel to each other because in doing so, the energy within the system was reduced.

In a small, applied field, a set of magnetic moments would experience that external field as well as an extra aligning field, due to the presence of the other magnetic moments. This extra field is proportional to the magnetization of the material.

Weiss also postulated that ferromagnetic materials consist of many smaller regions or domains,

containing similarly aligned magnetic moments, with the net magnetic moment of these domains being randomly oriented. This greatly increases the potential for large external magnetic moments. On the application of a field, these domains become aligned, parallel to the field.

This ferromagnetic ordering will break down at some critical temperature, known as the Curie point, due to the randomizing of parallel alignment with temperature. Above the Curie point, these materials become paramagnetic.

3.2. Antiferromagnetism

The origin of antiferromagnetism is similar to that for ferromagnetism. The difference is that while the atomic coupling in ferromagnetic materials occurs in parallel, in antiferromagnetic materials, the coupling is anti-parallel, and thus the net magnetic moment is zero. The susceptibility of such materials is very small and positive. The analogous point at which these couplings are destroyed due to thermal agitation is known as the Néel temperature. Above this temperature, antiferromagnetic materials are paramagnetic.

3.3. Ferrimagnetism

Ferrimagnetic materials exhibit characteristics of both ferromagnetic and antiferromagnetic materials. The magnetic moments of the coupled atoms are anti-parallel but unequal in magnitude; therefore there is a net overall magnetization. The susceptibility is small and positive. The iron oxide materials used in magnetic beads for HGMS systems are examples of ferrimagnetic materials. The imbalance in moments is caused by the presence of Fe ions in different oxidation states.

3.4. Diamagnetism

When an atom has core electrons in filled shells, and is subjected to an applied magnetic field, these 'core' electrons resist any tendency to align electron spins. This gives rise to core diamagnetism and is a manifestation of Lenz's law, which states that induced current flows always in a direction as to oppose the change causing it. The diamagnetism

produced gives a slight reduction in the magnetic flux present; diamagnets have a very small and negative susceptibility, in the order of -10^{-6} to -10^{-3} . Often the small magnetic moment in the material resulting from diamagnetism is masked by a larger paramagnetic effect.

3.5. Paramagnetism

In the absence of an external magnetic field, the electron energy bands of a paramagnetic material are equally populated with spin 'up' and spin 'down' electrons. Once a magnetic field is applied, there is an imbalance of electrons due to the presence of unfilled bands, and a weak magnetic effect is observed as the net magnetic moments are aligned in the field. Paramagnetic materials exhibit typical susceptibilities of 10^{-6} – 10^{-1} . This paramagnetic effect has a temperature dependence, since the magnitude of the induced magnetic field is limited by randomization due to thermal agitation within the atom. Paramagnetic materials lose their magnetic properties immediately when the external magnetic field is removed.

4. Magnetic circuit design

As described above, ferromagnetic materials contain domains. Within these, the spontaneous magnetization present is equal to the saturation magnetization of the material, and so the individual domains are fully magnetized at all times. In the absence of an applied field, there is no net magnetic moment or field generated by the material because the magnetization direction of each domain is randomly oriented.

During magnetization of the material, domains whose magnetization directions have a component in the direction of the applied field will grow at the expense of those that do not. Once domain wall movement has eliminated all of the unfavorably oriented domains, the magnetization direction of the single domain that remains will be rotated to be parallel to that of the applied field (see Fig. 1).

During magnetization, an increasing magnetic field is applied to the material until a saturation point is reached. Upon removing this applied field,

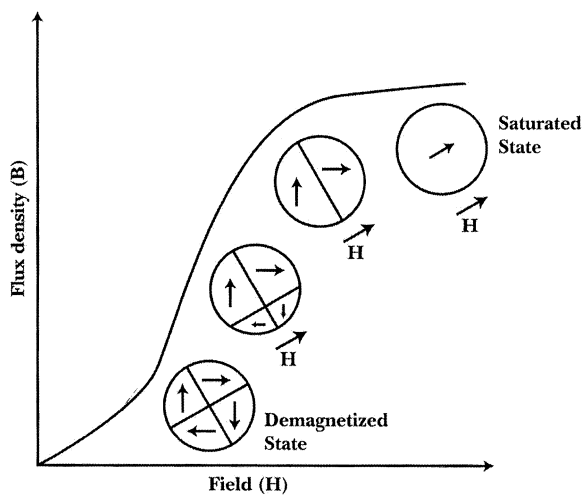


Fig. 1. Effect of applied field on the domain structure of a typical ferromagnetic material (after Jiles [1]).

a permanent magnet material will not follow the same path down to flux density = 0 — instead, it will retain some of its magnetism. The path that the permanent magnet follows is called a hysteresis loop and is a key tool in the quantitative analysis of permanent magnet performance in magnetic circuits such as those found in HGMS systems.

These loops are a graphical representation of the relationship between an applied magnetic field and the resulting induced magnetization within a material. Engineers sometimes use the polarization J of a magnet instead of its magnetization M when looking at magnetization, where

$$J = \mu_0 M. \quad (6)$$

The $B : H$ curve is known as the normal curve, while the $M : H$ curve is called the intrinsic curve. Examples of the hysteresis loops depicted by these curves are shown in Fig. 2. They show the properties of the magnetic material as it is magnetized and demagnetized. The second quadrant of each loop displays the magnetic properties of the magnet as it operates in a circuit, such as those found in HGMS systems. By comparing the second quadrant to known parameters within a given magnetic circuit, an approximation of the magnetic output can be determined. The second quadrant also represents the energy output of the magnet and is used extensively during magnet design.

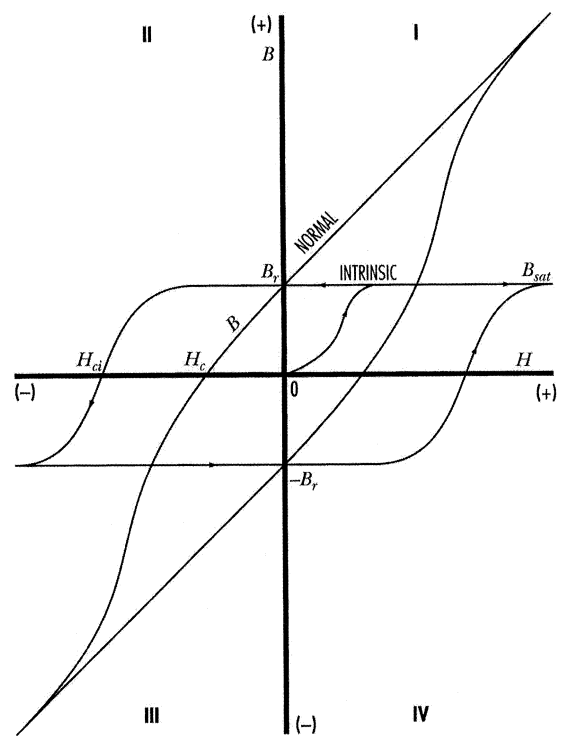


Fig. 2. The hysteresis loop.

When a magnetic field is applied to unmagnetized material, the intrinsic induction B is established within it, parallel to the applied field. If H is sufficiently strong, the magnet will become fully magnetized at the saturation flux density (B_{sat}). When the field is reduced to zero, the magnet will recoil to the residual value or remanence (B_r), as long as the magnet is within a closed magnetic circuit. Unlike soft (non-permanent) magnetic materials, the absence of an external magnetic field does not lead to demagnetization.

The permeability of a material was defined in Eq. (2). Note that this is dependent on circuit geometry, not magnetic properties. A key parameter that relates the geometry of a particular magnet to its magnetic properties is the permeance coefficient [defined in more detail later in the present work]. The magnetic characteristics of a particular magnet can then be evaluated by adding a line [known as the load line] to the second quadrant demagnetization curve, drawn from the origin, with a gradient equal to the negative of the permeance coefficient.

The intersection of the load line and the second quadrant demagnetization curve is called the operating point, where B_m and H_m for that geometry are determined, as shown in Fig. 3. Long thin magnets will have higher permeance coefficients [and thus a steeper load line] than shorter, disc-shaped magnets.

If a demagnetizing field is introduced into the system (e.g. from an electromagnet or another permanent magnet), the net magnetic field generated by the magnet is reduced in response to the demagnetizing field. The operating point of the magnet in the second quadrant of the hysteresis loop moves to the left. If the magnet is in a closed circuit, and this applied field reaches the value at H_c , there will be no net magnetization. This value is known as the normal coercivity. Ultimately, when the applied field reaches the value H_{ci} (known as the intrinsic coercivity), the magnet is completely demagnetized. These coercivity values are a measure of the magnet's ability to resist demagnetization.

The maximum product of the values of B and H for these curves gives the designer a value called the maximum energy product, BH_{max} . This is a commonly used figure of merit to compare different magnetic materials. The Nd-Fe-B materials exhibit the highest BH_{max} values to date, although

as stated above, other considerations should also be used when choosing a material for use in separator designs. Since there are two sets of units commonly used in magnetics, deriving from c.g.s. and MKS-SI unit systems, Table 2 shows a list of the common magnetic quantities and the conversion factors between units.

A magnetic circuit can be analyzed using techniques somewhat analogous to electrical circuit analysis. However, there is one critical difference that complicates magnetic circuit design. Since there is no perfect 'magnetic insulator', one must always account for leakage and fringing in the circuit design. HGMS systems must therefore be designed according to the 8 magnetic 'axioms' described in Table 3. Careful consideration of these axioms will clearly show the causes of leakage and fringing flux in a separator system design. The dichotomy between 'path of least resistance' in Axiom 1 and 'repulsion of lines' in Axiom 2 provides the explanation for fringing effects. Axioms 1, 4, 7 and 8, readily explain leakage effects.

The often unexpected and unwanted increase in leakage and fringing effects resulting from improper design or other circuit elements is explained by Axioms 7 and 8. For example, pole pieces with inadequate cross sections of unnecessary lengths or improper shapes result in a substantial increase in 'losses' at the expense of a working air gap flux.

A magnetic circuit is made up of one or more magnets and often there is some soft magnetic material to conduct the flux. When no soft magnetic material is present, the magnet is said to be in open circuit, and this is the case for most HGMS systems. On the other hand, when soft magnetic material forms at least one closed loop that conducts flux, the magnet is in a closed circuit. In order to do useful work, a magnetic circuit normally has one or more air gaps where the useful action is performed — in the case of HGMS systems, these air gaps will be the location where the magnetic particles and the entities to be captured are located.

The load line or permeance coefficient for a magnet is wholly dependent on its geometry, not on its intrinsic magnetic properties [2]. The permeance coefficient is directly related to the effective pole surface of the magnet, as well as its pole area. The pole surface is half of the total surface area of

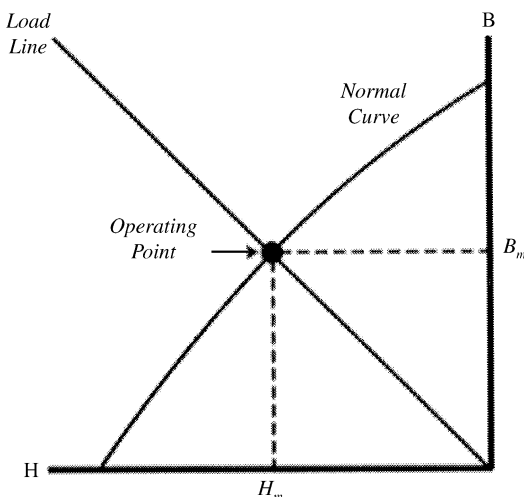


Fig. 3. Graph to show the relationship of the operating point of a magnet to its load line in the second quadrant of the hysteresis loop.

Table 2

Units and conversion factors for commonly used magnetic quantities

Quantity	Symbol	cgs unit	SI unit	Conversion factor (cgs unit/SI unit)
Permeability of free space	μ_0	Unity	$\text{WbA}^{-1}\text{m}^{-1}$	$1/(4\pi) \times 10^7 \text{ Wb}^{-1}\text{Am}$
Magnetic induction	B	G	T	$1 \text{ G} = 10^{-4} \text{ T}$
Magnetic field strength	H	Oe	Am^{-1}	$1 \text{ Oe} = 79.58 \text{ Am}^{-1}$
Unit mass magnetization	M	$\text{erg Oe}^{-1}\text{g}^{-1}$	$\text{JT}^{-1}\text{kg}^{-1}$	$1 \text{ erg Oe}^{-1}\text{g}^{-1} = 1 \text{ JT}^{-1}\text{kg}^{-1}$
Volumetric susceptibility	χ	Unity	Unity	$1/(4\pi)$
Maximum energy product	BH_{\max}	MGOe	kJ m^{-3}	$1 \text{ MGOe} = 7.958 \text{ kJ m}^{-3}$

Table 3

The 8 axioms of magnetic design

The eight axioms of magnetic design

1. Flux lines will always follow the path of least resistance. In magnetic terms, this means that flux lines will follow the path of greatest permeance.
2. Flux lines repel each other if their direction of flow is the same.
3. As a corollary to Axiom 2, flux lines can never cross.
4. As a corollary to Axiom 1, flux lines will always follow the shortest path through any medium. They therefore can only travel in straight lines or curved paths, and they can never take true right-angle turns. Meeting the terms of Axiom 2, flux lines will normally move in curved paths; although over short distances, they may be considered straight for practical purposes.
5. Flux lines will always leave and enter the surfaces of ferromagnetic material at right angles.
6. All ferromagnetic materials have a limited ability to carry flux. When they reach this limit, they are saturated and behave as though they do not exist (like air, aluminum and so on). Below the level of saturation, a ferromagnetic material will substantially contain the flux lines passing through it. As saturation is approached, because of Axioms 1 and 2, the flux lines may travel as readily through the air as through the material.
7. Flux lines will always travel from the nearest north pole to the nearest south pole in a path that forms a closed loop. They need not travel to their own opposite pole; although they ultimately do if poles of another magnet are closer and/or there is a path of greater permeance between them.
8. Magnetic poles are not unit poles. In a magnetic circuit, any two points equidistant from the neutral axis function as poles, so that flux will flow between them (assuring that they meet the other Axioms stated above).

the magnet, whereas the pole area is the area of the end face of the magnet. This is an approximation based on a spherical magnet, and it breaks down when the magnet is very long — however, it is

a good approximation for the types of magnets used in HGMS systems.

The relevant equation is thus:

$$\frac{B}{H} = (\sqrt{\pi s}) \frac{L_m}{A_m}, \quad (7)$$

where L_m is the magnet length, A_m the pole area, and s the pole surface.

From this concept, other equations can be derived for specific geometries such as rectangles and cylinders. Using the Biot–Savart law, which determines the magnetic field contribution of a current carrying element, it is possible to calculate the flux density along the axis of a permanent magnet of simple shapes. Only the dimensions and residual induction (B_r) of the material are required. This approach equates permanent magnets to solenoids (or current sheets) with the same shape. These equations are very useful tools for permanent magnet design. Note that the direction of flux will be normal to the pole surface along the axis.

One such equation can be used for cylindrical magnets (as shown in Fig. 4)

$$B = \frac{B_r}{2} \left[\frac{d+1}{\sqrt{(d+l)^2 + r^2}} - \frac{d}{\sqrt{d^2 + r^2}} \right], \quad (8)$$

where B is the flux density at a point d away from the pole face [parallel to the axis of the cylinder], B_r is the remanence or residual induction of the magnetic material being used, r is the radius of the cylinder and l is its length.

It should be noted that d can be a negative value — i.e. one can determine the value of B within the magnet material itself. From empirical results, the value obtained for $d = -0.5l$ should give

a good approximation of the flux density of the magnet at its operating point, when compared to the B_m value for the second quadrant demagnetization curve for the material (see Fig. 3). Also note that any units for dimensions can be used.

This equation can be used to compare magnet geometries of the same volume, and the effect that these dimensions will have on the separator systems being developed. One geometry configuration may generate a strong flux density close to the pole

face, but may be very weak at a distance — while another may have a weaker flux density close to the pole face, but will have more ‘reach’ and have higher values of flux density further away from the pole.

Eqs. (7) and (8) were used to generate the graphs that appear in Figs. 5 and 6. A material with B_r of 1000 mT was used in the calculations. The variable d (the distance from the pole face at which flux density is calculated) was set to 0.5 of the magnet length. Altering the diameter and length of the magnet, while conserving the unit volume of the magnet, is a good method of determining the optimum dimensions for a cylindrical magnet.

Fig. 5 shows that increasing the length of a magnet will increase the flux density at its pole face, but will decrease the flux density away from the pole face much more quickly than for shorter, more ‘stubby’ magnets. In other words for the same volume of material, long, thin magnets have a higher strength at their pole faces, but they do not have as much reach as shorter ‘stubby’ magnets. In the case of the magnet used in Fig. 5, the average between these two values will give an indication of the optimum magnet geometry to make best use of the material for a given unit volume. In this case,

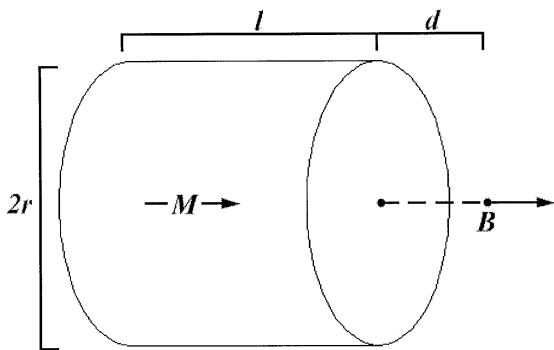


Fig. 4. Dimensions of a cylindrical magnet used to calculate flux density at a distance from the pole face.

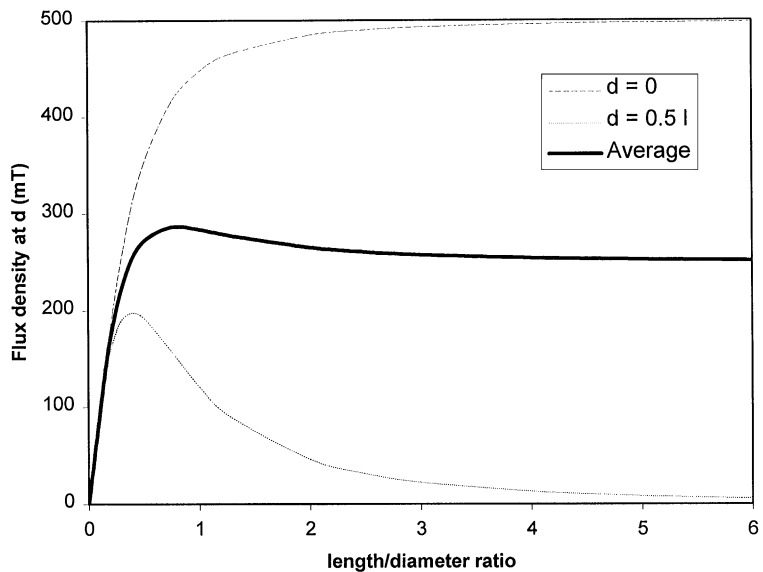


Fig. 5. Graph to show relationship of the length/diameter ratio to the resulting flux density at a distance, d , from the magnet pole face for a cylindrical magnet with B_r of 1000 mT.

the optimum value was obtained for a length/diameter ratio of 0.737 as shown in Fig. 5. This gives dimensions (any units) of $r = 0.600$ and $l = 0.885$ for a unit volume.

Fig. 5 also shows that the benefits from making a magnet longer diminish quickly. The flux density at the pole face of the magnet converges asymptotically to a value of 500 mT, or a value of half the B_r . This is to be expected from the presence of the $B_r/2$ term in Eq. (8).

Fig. 6 shows a quick way to determine the permeance coefficient of a cylindrical magnet based on its length/diameter ratio. Many other curves for different geometries (including rectangular blocks and rings) have been published [2]. The authors' company has also made many other equations, curves and other design data freely available in the form of a complimentary Reference and Design Manual, available at the above address [3]. Such data will show that there is an optimum shape for all magnet geometries.

The above equations can be used to generate spreadsheets that will allow the user to design simple separators by making d equal to the far side of the interior wall of the vial or container used for separation. Appendix A lists the appropriate equations that can be entered into an Excel or other spreadsheet, to generate data that can then be plotted as a graph, and an optimum design chosen. The

spreadsheet can be freely obtained from the authors at the address above.

5. Considerations specific to separator unit design

All magnetic separation is based on a source of magnetic flux inducing a magnetic moment in the target to be captured. The value of the magnetic moment in the source, and the target, is the product of their respective pole strength and the inter-polar distance. Pole strength in the source is the total flux produced; this value is determined by magnetic properties and geometry. Pole strength in the target is the total number of magnetic flux lines induced in it. The inter-polar distance is often difficult to measure precisely, but its value is not really needed unless derivation of unit properties is the goal.

Coulomb found that the force exerted between magnets is proportional to the product of pole strengths and inversely proportional to the square of the distance between the poles. Since magnetic point poles do not exist, the effect between both poles in the source on both induced poles in the target must be considered. However, the particles used for HGMS are much smaller than the distance between the poles of the source, so the point value of flux density at the location of the particle can be used here.

The value of flux density in space diminishes with the square of the distance from the source magnetic poles. Sources with great distances between their poles will then tend to have a 'dog bone' field about them, and particles will see a greater attractive force near the poles. When the distance from particle to pole greatly exceeds the source pole spacing, the force on a particle will diminish as the cube of the distance. Values are not important here, but it should be apparent that magnetic capture efficiency is much greater when the target is closer to the source than one-half of the source pole spacing. The magnetic gradient will also be greatest in a mid-plane normal to magnetic axis of the source.

In tramp iron separators, the properties and geometry of the targets contribute to system efficiency. Long objects with a high magnetic permeability see the source field as a magneto-motive force (mmf), which gives rise to an induced magnetic field in the

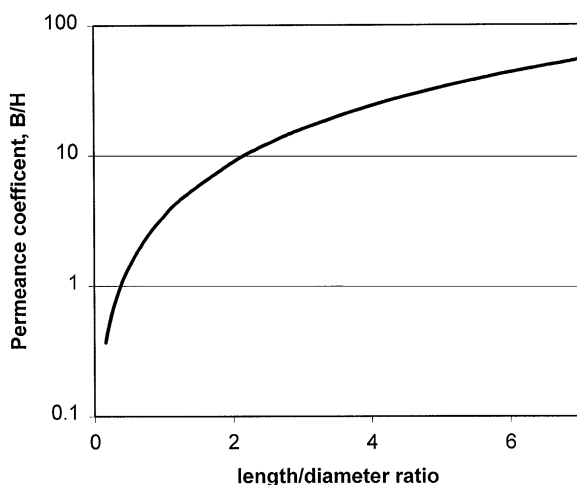


Fig. 6. Graph to show relationship of the length/diameter ratio to the permeance coefficient of cylindrical magnet.

target object. Because the mmf increases as the source is approached, and the induced field strength increases with mmf, there is a non-linear acceleration of the object toward the source. If the object length and position are such that it gives source flux a preferred low reluctance path between its own poles this effect is maximized. This favorable effect occurs when several smaller objects join together, because of the polarity of their induced fields, and act like a longer object to give source flux a more desirable path. Tramp iron separators have other physics to contend with, like magnetic properties and viscosity of the medium, and gravity.

Macro separation systems function in a similar manner. The classic example of iron filings in a magnetic field vividly illustrates what takes place. Iron particles build up initially at the source poles and extend toward each other as separation continues to connect the induced north and south poles in the filings. When the source is removed, some of these particles may cling together for long periods because their combined geometry produces enough anisotropy to retain some level of magnetization until shock or temperature overcome this effect. As described below, such an effect would be undesirable in the magnetic particles used for HGMS systems, since the lack of a magnetic memory is essential to the process. In addition, the typical magnetic bead does not have a high concentration of magnetic material (the rest typically being a polymer or protein carrier), so they do not form a more efficient combined geometry as they are attracted to source poles.

Because these particles have no intrinsic permanent magnetic properties, and induction is so low, they contribute little to the efficiency of the magnetic system. The properties of the magnetic field source are therefore dominant in the separation process.

Sizing and arranging magnets for each system as described above achieves improvements in the shape and strength of a source magnetic field. Further optimization of field strength and gradient are possible by combining magnets with their orientations in quadrature, taking advantage of the principle of superposition. In quadrature arrangements, the coercivity of the material used must be greater

than the fields generated to avoid demagnetizing portions of the adjacent magnet. Such utilization of superposition in the design of permanent magnet sources has only recently become practical, with the availability of modern high-coercivity materials.

It has been shown [4–6] that in an applied magnetic field, the force on the particles can be approximated by

$$\mathbf{F} = \frac{1}{2} \frac{\chi V_p}{\mu_0} \nabla(B^2), \quad (9)$$

where χ is the difference in susceptibility between the particle and the fluid, V_p is the volume of the particle and B is the magnitude of the flux density, equivalent to the magnetic field, $\nabla(B^2)$ is the part of the equation dependent on the magnetic field. Since

$$\nabla(B^2) = 2(\mathbf{B} \cdot \nabla)B \quad (10)$$

the resultant force on a particle in a magnetic field is proportional to the strength of the magnetic field, and to the field gradient that the particle experiences. The $(\mathbf{B} \cdot \nabla)B$ portion of Eq. (10) is called the magnetic force density. Since the size of the particle is very small in comparison to the inter-polar distance, a point value can be used to closely approximate the effects experienced by the particle.

At any point on a plane within the active volume of the separator, we can approximate the gradient of field \mathbf{B} at point (x, y) by averaging the change in field between point (x, y) and its neighbors, as illustrated in Fig. 7, and described as follows:

$$\frac{\partial B(x, y)}{\partial x} = \frac{B_{(i-1, j)} - B_{(i+1, j)}}{2}, \quad (11)$$

$$\frac{\partial B(x, y)}{\partial y} = \frac{B_{(i, j-1)} - B_{(i, j+1)}}{2}. \quad (12)$$

Such values can be obtained by mapping the magnetic field within the separator or by modeling such systems in boundary or finite element analysis packages. The calculated flux density in the bore [diameter = 7 mm] of a typical quadrupole separator is shown in Fig. 8a, as generated by Magneto, a 2D boundary element modeling package. Fig. 8b shows the flux lines within the bore of the quadrupole. Using Eqs. (11) and (12), we can then plot the magnetic force density in the operating gap as shown in Fig. 8c [low values in the middle, higher

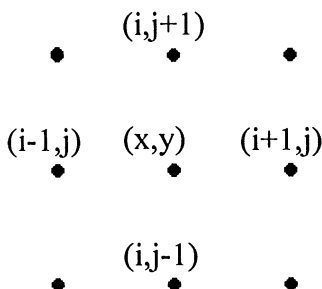


Fig. 7. (x,y) and neighboring coordinates used to calculate field gradient in a plane.

values towards the magnets — note that the range of values in this plot is relative to the range shown in Fig. 8a].

It can be seen that the general profile of the force density plot does not differ much from the \mathbf{B} plot. Since there is a similarity in the type of information shown in Figs. 8b and c, most comparisons between separator designs can be made by looking simply at the flux density plot. However if one is not sure which separator design will produce a faster separation (through increased force acting on the particles), force density values can be summed for the area of interest for quantitative comparison. This is illustrated by comparing the results shown in Fig. 8, with those for an improved patent-pending quadrupole configuration [7] shown in Fig. 9. Zborowski et al. [4] showed that the magnetic force acting on a magnetized particle in an ideal quadrupole has a centrifugal character. It can clearly be seen that the improved quadrupole design in Fig. 9 produces a higher magnetic force density, resulting in a more efficient field source and faster separation time than the classic quadrupole design.

This technique also answers decisively the question of the effectiveness of using a high-field dipole for similar separations. While B is very high in these systems, $(\mathbf{B} \cdot \nabla)B$ is quite low. A larger mass of permanent magnet material is required to generate the same force density sum as that which can be obtained from a quadrupole.

For such *closed* structures, a $2n$ -pole ($n = 2, 3, 4, \dots$) structure gives the best results for HGMS systems. Using magnets in quadrature to maximize \mathbf{B} , and which have a null point in the

middle to maximize $(\mathbf{B} \cdot \nabla)B$ makes for the most efficient use of magnet material. Such systems will lend themselves well to continuous magnetic separation systems [4], but not so well to automated discrete tube-based tests, and so a natural extension of this technique would be to analyze open linear structures designed to act upon test tube racks.

6. Particle material considerations

The primary evaluation process for selecting the appropriate magnetic particles for use in an HGMS system will naturally center around the ligands and other binding coatings that are attached to the particles, which will be customized to match the specific entity being targeted for capture. However, the manufacturers of such particles have to take into account the underlying properties of the particles, which act as a substrate to the biochemistry that occurs at the particle surface. Although it is the presence of active ligands and other coatings that ultimately interact with the entities being captured, it is the specific magnetic and physical characteristics of the substrate particle that will determine the time for separation, its efficiency and retention rate.

Most of the magnetic particles used in HGMS systems have some form of iron oxide at their core. Typically these iron oxide phases are ferrimagnetic in the monolithic form (see Table 4), but when particles are manufactured from bulk material, and the diameter of these particles is carefully controlled, a distinctly different magnetic phenomenon is observed.

By reducing the particle size to below some critical diameter, the particles become so small that the magnetic moments present in each particle (by virtue of the underlying ferrimagnetism inherent to the material) are constantly being re-oriented by random thermal energy vectors in the system (even in ambient conditions). Thus the particles have a coercivity (ability to resist demagnetization) of zero and the net magnetic moment of the powder is zero. The bulk powder is thus essentially ‘non-magnetic’.

However, the particles are still susceptible to applied magnetic fields, and in this regard they are

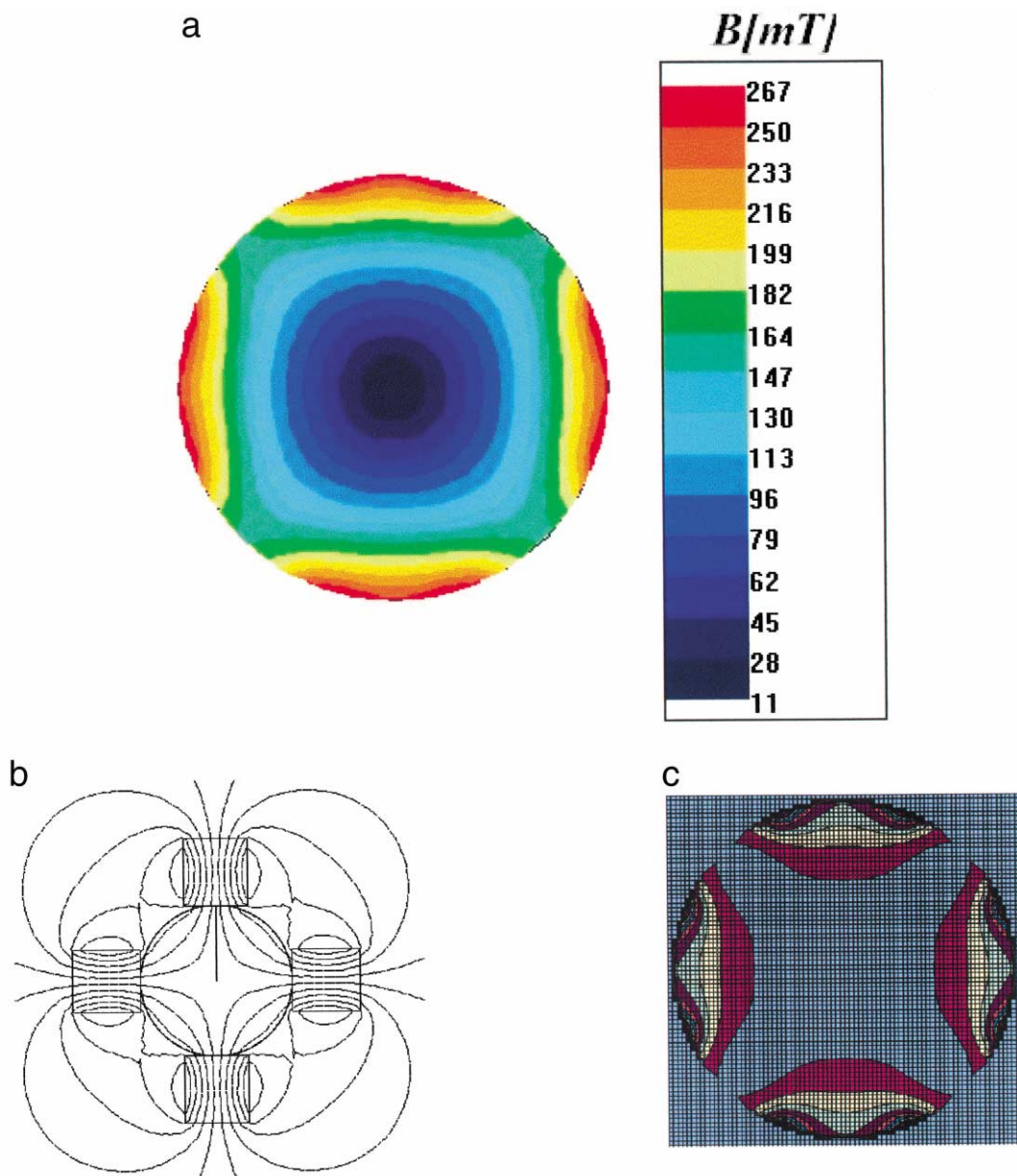


Fig. 8. (a) Flux density [magnitude] plot in bore of classic quadrupole magnet [diameter = 7 mm]. (b) Flux line plot for classic quadrupole magnet. (c) Force density plot in bore of classic quadrupole magnet.

similar to paramagnetic materials. Because of the presence of so many large magnetic moments within the individual powder particles, the susceptibility of the powder is very large, and thus the particles behave like ‘super’ paramagnets. Removing the ap-

plied magnetic field from the particles will instantaneously reduce the overall net magnetic moment of the powder back to zero. Thus, the powder has no ‘magnetic memory’, and it is possible to use these particles within a system that uses a number

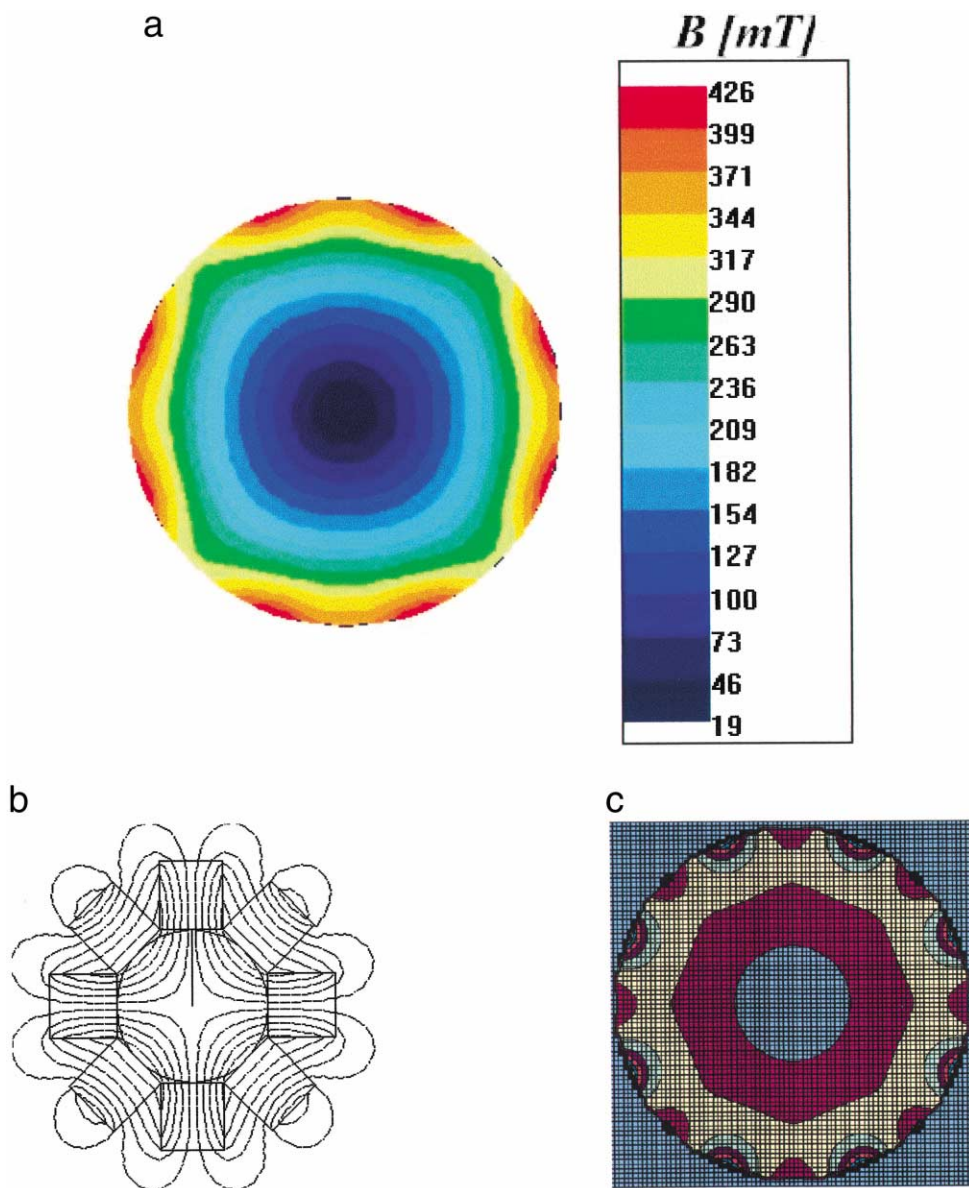


Fig. 9. (a) Flux density [magnitude] plot in bore of improved quadrupole magnet [diameter = 7 mm]. (b) Flux line plot for improved quadrupole magnet. (c) Force density plot in bore of improved quadrupole magnet.

of recurring separation cycles. The superparamagnetic limit or particle diameter, below which this phenomenon is observed, is usually in the 1–30 nm range.

If the particles are slightly larger than their superparamagnetic limit diameter, the time for ran-

domization of the magnetic moments will become discernible. Kötitz et al. [8] discuss the additional influence of Brownian motion on this process.

It is important to note that this superparamagnetic limit diameter is material-specific. Particles

Table 4
A summary of common iron-based oxide and hydroxide compounds

Mineral name	Composition	Common chemical name	Mass susceptibility χ
Wustite (rust)	FeO	Ferrous oxide	$\sim 2 \text{ JT}^{-1} \text{ kg}^{-1}$
Hematite	$\alpha\text{-Fe}_2\text{O}_3$	Ferric oxide	$\sim 1 \text{ JT}^{-1} \text{ kg}^{-1}$
Maghemite	$\gamma\text{-Fe}_2\text{O}_3$	Ferric oxide	$\sim 70 \text{ JT}^{-1} \text{ kg}^{-1}$
Magnetite	Fe_3O_4	Ferrous-ferric oxide	$\sim 90 \text{ JT}^{-1} \text{ kg}^{-1}$
Goethite	$\alpha\text{-FeO-OH}$	Ferrous hydroxide	
Akaganéite	$\beta\text{-FeO-OH}$	Ferrous hydroxide	
Ferroxyhite	$\delta\text{-FeO-OH}$	Ferrous hydroxide	
Lepidocrocite	$\gamma\text{-FeO-OH}$	Ferrous hydroxide	
Limonite	$\alpha\text{-FeO-OH} + \gamma\text{-FeO-OH}$	Hydrated ferrous oxides	

with a diameter larger than this limit become resistant to the thermal demagnetization effects outlined above, and thus will exhibit an undesirable ‘magnetic memory’ after being exposed to an applied magnetic field. However, as shown above, in order to maximize the force upon magnetic beads within the applied magnetic field (which leads to an increased velocity of the particles and a reduced separation time), individual bead size should be as large as possible.

The system designer must therefore balance the need to eliminate magnetic memory within the particles, with the need to minimize separation time during the separation process. This is usually achieved by mixing quantities of nanophase magnetic particle crystals with a protein or polymer (e.g. polystyrene, silane or dextran), to form a magnetic bead, that is then coated with activated target capture coatings that are specific to the target entities to be captured (e.g. avidin). Manufacturers can alter the fraction of magnetic media within each magnetic bead to control the separation behavior *in situ*.

In addition, the active surface area of the particle needs to be as large as possible in order to maximize target capture and retention of the biological entities being captured. Altering the smoothness of the final surface of the particles allows the particle manufacturer to control the active surface area of the powder being used.

Materials with a high magnetic anisotropy will require crystals with a smaller diameter than isotropic particles, in order to get below

the superparamagnetic limit. Some factors of the overall anisotropy are material-specific, but the shape of a given magnetic particle will also affect the magnetic anisotropy. A spherical particle will minimize this anisotropy and such a particle is also less likely to retain magnetism once an applied field has been removed. However, this benefit is offset by the slightly reduced polarization of such particles when a field is applied, which will affect the velocity of the particle’s movement within the liquid medium of the HGMS system. The reduction in anisotropy is usually the dominant factor, and thus the ideal magnetic bead will generally be spherical, and contain iron oxide crystals with low aspect ratios and average diameters in the 1–30 nm range to achieve superparamagnetism.

Additional methods to decrease the separation time and to improve yield and efficiency include those that utilize an oscillating magnetic field, through the movement of the magnets surrounding the magnetic particles. In addition, the particle container can be rotated [9] in cycles to allow for better mixing of the particles within the mixture containing the target entities, without damaging them.

Acknowledgements

The authors wish to thank Mr. Ging-Li Wang, Mr. Richard Bennett, Mr. Bruce Toyama and Mr. Jeff Foy, all of Dexter Magnetic Technologies, for useful discussions.

Table 5

Equations for spreadsheet calculations of flux density for cylindrical magnets

A 1 Value	B Equation or value	C Example
2 Remanence of material, B_r (mT)	See published data	1000
3 Radius of magnet, r	Set for particular magnet	0.6
4 Distance from pole face, d	Set for particular container diameter	0.442097
5 Length of magnet, L	Set for particular magnet	0.884194
6 $d + L$	= B4 + B5	1.326291
7 Volume	= B3^2*PI()*B5	1
8 L/D	= B5/2/B3	0.736828
9 B/H	= 1.77*B5/B3^2/PI()*(B3^2*PI() + PI()*B3*B5)^0.5	2.314538
10 B_{gap} at pole face (mT)	= 0.5*B2*((B5/(B5^2 + B3^2)^0.5))	413.735
11 B_{gap} at d (mT)	= 0.5*B2*((B6/(B6^2 + B3^2)^0.5 - B4/(B4^2 + B3^2)^0.5))	158.957
12 Average B_{gap} (mT)	= (B10 + B11)/2	286.34
13 B_{gap} ratio	= B11/B10	0.384199

Appendix A. Spreadsheet equations for determining flux density for a cylindrical magnet

Table 5 shows the necessary spreadsheet calculations needed to utilize Eqs. (7) and (8) for determining the magnetic flux density within a simple separator unit. By setting the value of d to the diameter of the container [for example a 15 or 50 ml tube], and choosing appropriate dimensions for the magnet, the reader can determine the flux density within their system, and create their own plot similar to Fig. 5.

By using different values of d for the same magnet, the user can also create a graph of flux density from one side of the container at the pole face [$d = 0$] to the other side of it. By dividing the flux density by the distance across the container, the reader can then determine the average flux density gradient across the unit. The spreadsheet for these equations may also be obtained from the authors at the address above.

References

- [1] D. Jiles, Introduction to Magnetism and Magnetic Materials, Chapman & Hall, London, 1991.

- [2] R. Parker, R. Studders, Permanent Magnets and their Application, Wiley, New York, 1964.
- [3] Dexter Magnetic Technologies [a.k.a. Permag Corp], Reference and design manual, 1998 [available from the authors' company by email or surface mail].
- [4] M. Zborowski, L. Sun, L. Moore et al., *J. Magn. Magn. Mater.* 194 (1999) 224.
- [5] R. Gerber, R. Birss, in: High Gradient Magnetic Separation, Wiley, New York, 1983, p. 69.
- [6] R. Parker, Advances in Permanent Magnetism, Wiley, New York, 1990.
- [7] Genzyme Corp and Permag Corp [a.k.a. Dexter Magnetic Technologies], 1998, WIPO application # PCT/US98/11816.
- [8] R. Köttitz, W. Weitschies, L. Trahms et al., *J. Magn. Magn. Mater.* 194 (1999) 62.
- [9] Sigris Research Inc, 1996, WIPO application # PCT/US96/02212.

Further reading

Bibliography

- R. Bozorth, Ferromagnetism, Van Nostrand, Princeton, 1968.
- J.M.D. Coey (Ed.), Rare-earth Iron Permanent Magnets, Clarendon Press, Oxford, 1996.
- J.D. Livingstone, Driving force — the natural magic of magnets, Harvard University Press, Cambridge, 1996.
- J.A. Stratton, Electromagnetic Theory, McGraw-Hill, New York, 1941.